Algal Research 31 (2018) 387–394

Contents lists available at ScienceDirect

Algal Research

journal homepage: www.elsevier.com/locate/algal

The impact of day length on cell division and efficiency of light use in a starchless mutant of *Tetradesmus obliquus*

G. Mitsue León-Saiki[a,*], Tània Cabrero Martí[a], Douwe van der Veen[a], René H. Wijffels[a,b], Dirk E. Martens[a]

[a] Bioprocess Engineering, AlgaePARC, Wageningen University and Research, P.O. Box 16, 6700 AA Wageningen, The Netherlands
[b] Faculty of Biosciences and Aquaculture, Nord University, N-8049 Bodø, Norway

ARTICLE INFO

Keywords:
Microalgae
Scenedesmus obliquus
Day/night cycle
Cell division
Diurnal biochemical changes
Photosynthetic efficiency

ABSTRACT

Large scale microalgal production will be primarily done under natural sunlight conditions, where microalgae will be exposed to diurnal cycles of light and dark (LD) and to differences in the length of both periods (photoperiod). *Tetradesmus obliquus* (formerly known as *Scenedesmus obliquus*), a strain with potential for biofuel production, and the starchless mutant *slm1* were grown under 3 different LD periods: 16:8 h, 14:10 h and 12:12 h. Cell division started a fix number of hours after the light went on (sunrise), independently of the length of the photoperiod. For the wild-type, cell division started approximately 14 h after the beginning of the day and occurred mainly at night. For the starchless mutant *slm1*, timing of cell division was also independent of the photoperiod length (starting 10–12 h after sunrise). However, as opposed to the wild-type, cell division always started during the day. For both strains, growth rate increased with increased length of the light period. The *slm1* mutant is capable of surviving long dark periods (up to 12 h) despite the lack of starch. In general, the *slm1* mutant has a lower photosynthetic efficiency than the wild-type, with the 12:12 h LD resulting into even less efficiency than the other two LD cycles.

1. Introduction

Microalgae can be used as source for commercial products of interest such as biofuels, chemicals, food, and feed [1,2]. Large scale microalgal production will be primarily done under natural sunlight conditions [3,4], where microalgae will be exposed to diurnal cycles of light and dark (LD). Diurnal LD cycles are ubiquitous and many organisms synchronize their metabolism to anticipate the changing environment [5–9]. Environmental cues (known as Zeitgeber, which is German for time indicator) entrain the internal timing to a period of 24 h [8,10]. Cues such as sunrise (dawn), sunset (dusk), changes in light intensity or temperature, as well as light pulses can be used to entrain this diurnal cycle [11]. For photosynthetic organisms, synchronization to the diurnal LD cycle translates into fine-tuning their photosynthetic apparatus to capture sunlight efficiently during the day and to schedule ultraviolet or oxygen sensitive processes (e.g. nitrogen fixation, DNA synthesis or cell division) at night [12–15]. In addition, the length of the light and dark periods under natural sunlight conditions varies depending on the region and the season, which has an impact on biomass productivity and photosynthetic efficiency [16] depending on the species.

The microalga *Tetradesmus obliquus* (formerly known as *Scenedesmus obliquus* [17] and reclassified as *Acutodesmus obliquus* [18]) is an industrially relevant strain whose potential has been demonstrated [19–22]. In addition, de Jaeger et al. [23] developed a starchless mutant, *slm1*, which is incapable of synthesizing starch due to a single nucleotide polymorphism in the small subunit of ADP-glucose pyrophosphorylase, the committed step of starch biosynthesis [24]. This mutant showed a higher maximum triacylglyceride (TAG) yield on light (0.217 $g \cdot mol_{ph}^{-1}$ compared to 0.144 $g \cdot mol_{ph}^{-1}$ for its wild-type) and a higher maximum TAG content (0.57 $g \cdot g_{DW}^{-1}$ compared to 0.45 $g \cdot g_{DW}^{-1}$) in batch cultures under nitrogen starvation [25]. Furthermore, the photosynthetic efficiency of the mutant was comparable to the wild-type under nitrogen starvation.

Prior to the TAG producing step, which commonly takes place under nitrogen limitation/starvation and LD cycles, biomass must be grown under nitrogen replete conditions. Under nitrogen replete conditions, *T. obliquus* wild-type uses starch as a temporary energy storage compound

Abbreviations: LD, light/dark; mol_{ph}, mol of photons; DW, dry weight; OD_{750}, optical density at 750 nm; TAG, triacylglycerol; D, dilution rate; V_{PBR}, photobioreactor volume; μ_t, time-specific cell division rate

* Corresponding author.
E-mail address: graciela.leonsaiki@wur.nl (G.M. León-Saiki).

https://doi.org/10.1016/j.algal.2018.02.027
Received 31 October 2017; Received in revised form 16 January 2018; Accepted 22 February 2018

during LD cycles [26]. Thus, energy and carbon are stored during the day which are next used at night. When starch synthesis is blocked, as for starchless mutants, different effects on growth under nitrogen replete conditions are observed for different microalgae. However, most of the studies have been done under continuous light [27–30], which is not relevant for outdoor production. Furthermore effects of the absence of starch are expected to be more severe during LD cycles, since the algae use starch during the dark as a source of energy and carbon. To our knowledge, only one report of growth of the starchless mutant of *Chlorella pyrenoidosa* STL-PI was done under 12:12 h LD cycles, showing an increase in growth compared to its wild-type [28]. Additionally, as starchless mutants are made to improve TAG production, most studies on these mutants focus on their performance during the TAG producing step under nitrogen limitation or starvation conditions [22,25,27,29–31], and little is known about their diurnal behavior under nitrogen replete conditions and LD cycles. The diurnal cycles of the starchless mutant of *T. obliquus slm1* were studied under 16:8 h LD cycles, where this mutant showed synchronized growth and cell division even in the absence of starch or any other storage compound, albeit with decreased growth and energy efficiency compared to its wild-type [26]. However, as previously mentioned, production conditions outdoors will include variations in the light and dark periods and it is thus interesting to know how the mutant will react to these variations. Especially, it is interesting to know how the mutant will react to longer dark periods since a temporary energy storage compound is missing.

Therefore, the aim of this paper is to obtain insight into how a starchless mutant of *T. obliquus* copes with different LD periods as compared to its wild-type. For this, scheduling of cell division, energy efficiency and biomass composition were measured under 3 different photoperiods of typical day/night duration throughout the year for both the wild-type and the starchless mutant *slm1*.

2. Materials and methods

2.1. Strains, pre-culture conditions and cultivation medium

Wild-type *Tetradesmus obliquus* UTEX 393 (reclassified from *Scenedesmus obliquus* [17] and *Acutodesmus obliquus* [18]) was obtained from the Culture Collection of Algae, University of Texas. The starchless mutant of *T. obliquus* (*slm1*) was generated as described by de Jaeger et al. [23]. Liquid cultures of 100 mL of filter sterilized (pore size 0.2 μm) defined medium designed by Breuer et al. [19] were maintained in a culture chamber with shaker in 250 mL Erlenmeyer flasks (25 °C, 16:8 h light/dark cycles with 30–40 $\mu mol \cdot m^{-2} \cdot s^{-1}$, 150 rpm, air in headspace). Prior to the start of the experiments, cultures were placed in a shake incubator operating at 25 °C with continuous light (120 $\mu mol \cdot m^{-2} \cdot s^{-1}$) and a headspace enriched with 2.5% CO_2 to reach the desired inoculation cell density.

2.2. Reactor set-up and experimental conditions

T. obliquus was continuously cultivated in a sterile flat panel airlift-loop reactor with a 1.7 L working volume and a 0.02 m light path (Labfors 5 Lux, Infors HT, Switzerland). Reactor set-up, temperature, pH and airflow were set and controlled as described by León-Saiki et al. [26]. Light was provided at an incident photon flux density of 500 $\mu mol \cdot m^{-2} \cdot s^{-1}$ in 3 different light/dark (LD) block cycles: 16:8 h, 14:10 h, and 12:12 h. Cultivations were turbidostat controlled, where the culture was diluted with fresh medium when the light intensity at the back of the reactor dropped below the setpoint (10 $\mu mol \cdot m^{-2} \cdot s^{-1}$). The feeding was stopped during the dark period to prevent washing of the culture.

The reactor was inoculated at an optical density (OD_{750}) of 0.1. Cultures were allowed to reach steady state, which was defined as a constant biomass concentration and 24 h-dilution rate for a period of at least 3 residence times. After steady state was reached, liquid samples were freshly taken from the reactor and either immediately used for cell count (1 mL) and dry weight measurements (3 mL, in triplicate) or centrifuged for 5 min at 2360 × *g* for biochemical analysis (12 mL for proteins, 5 mL for starch, 5 mL for triacylglycerides (TAG) and 5 mL for total carbohydrates). For biochemical analysis, the resulting pellet was transferred to bead beating tubes (Lysing Matrix E; MP Biomedicals Europe) or glass tubes (for total carbohydrates analysis) and stored at −20 °C. Pellets were freeze dried and stored again at −20 °C until further analysis. Sampling was done in intervals of 1 h for cell counts. Biomass composition was analyzed in intervals of 3 h for the 14:10 h and 12:12 h LD. For the 16:8 h LD, biomass composition was obtained from a previous publication [26]. In addition, at least 3 daily overflow samples were collected for each photoperiod and strain.

2.3. Analyses

Dry weight (DW) concentration was determined in triplicate as described by Kliphuis et al. [32]. Starch was measured using a total starch kit (Megazyme, Ireland) as described by de Jaeger et al. [23] with the modification that 5 mg of freeze dried biomass was used for the analysis. Protein content was measured using a colorimetric assay (Bio-Rad DC protein assay) as described by Postma et al. [33] with the difference that 10–12 mg of freeze dried biomass was used for analysis. Triacylglycerol (TAG) content was determined as described by Remmers et al. [22]. Total carbohydrates were extracted and quantified according to DuBois et al. [34] and Hebert et al. [35].

2.4. Cell number and size

T. obliquus cells aggregate and form coenobia [36]. To separate the cells, a 1 mL cell suspension was sonicated on ice for 30 s at 30% amplitude using a probe sonicator (Sonics vibra-cell, USA). The absence of coenobia after sonication was verified under the microscope. Cell number and size were determined using a Beckman Coulter Multisizer 3 (Beckman Coulter Inc., USA). The sonicated culture was diluted 200 times with Isoton® II diluent solution. Cells with diameter above 2.5 μm were counted. As some cell counts were done only in duplicate (n = 2), we show the range of values measured by including the maximum and minimum values found.

2.5. Dilution rate, doubling time and time-specific cell division rate

Dilution rate (D_{24h} in day^{-1}) was calculated by logging the medium (feed) and acid consumption over 24 h (V_{24h} in L) and the volume of the photobioreactor (V_{PBR} in L) (Eq. (1)) [37]:

$$\mu_{24h} = D_{24h} = \frac{V_{24h}}{V_{PBR}} \quad (1)$$

Dilution rates over small intervals of time were calculated by logging the medium and acid consumption in intervals of 10 min, followed by a moving average per 60 min. Dilution patterns were repeated daily. Values corresponding to 1 h were averaged and used for the time-specific cell division rate (μ_t), which was calculated based on a cell number balance (C_{cells}) and D_t following:

$$\frac{dC_{cells}}{d_t} = -D_t \cdot C_{Cells} + \mu_t \cdot C_{Cells} \quad (2)$$

$$\mu_t = \frac{\frac{dC_{cells}}{d_t} + D \cdot C_{Cells}}{C_{Cells}} \quad (3)$$

Hourly values were added up to get the cumulative cell division rate. The average dilution rate over the light period was calculated by dividing the daily average dilution rate (D_{24h}) by the amount of hours of light supplied, with the following equation:

$$D_{over\ light\ period} = \frac{D_{24h} \cdot 24}{hours\ of\ light\ supplied} \quad (4)$$

The doubling time (t_d) was calculated as a function of the dilution rate (D), using the following equation:

$$t_d = \frac{ln\,2}{D} \quad (5)$$

2.6. Calculations

Biomass yield on light (in $g_{DW} \cdot mol_{ph}^{-1}$) was calculated as the ratio between the biomass productivity (in $g \cdot L^{-1} \cdot day^{-1}$) and the photon absorption rate (in $mol_{ph} \cdot L^{-1} \cdot day^{-1}$). Starch productivity (in $g \cdot L^{-1} \cdot h^{-1}$) was calculated using a balance for starch over short time intervals as explained by León-Saiki et al. [26]. The theoretical energy conversion efficiencies were calculated based on the theoretical photon requirements for the biomass components (3.24 $g \cdot mol_{ph}^{-1}$ for starch and 1.62 $g \cdot mol_{ph}^{-1}$ for functional biomass [32,38]) and the photon absorption rate [26]. Triacylglyceride (TAG) content remained below 1% and was omitted for this calculation. Samples were taken in intervals of 3 h in the 14:10 h LD and 12:12 h LD cycles. For the calculation of the hourly energy conversion efficiency in these 2 cycles, the additional points for biomass composition were estimated assuming a proportional change between the measured points.

3. Results and discussion

3.1. Growth rate under different light regimes

We started by characterizing growth of *Tetradesmus obliquus* wild-type and starchless mutant *slm1* under light/dark (LD) cycles of 16:8 h, 14:10 h and 12:12 h. Since the reproducibility of the turbidostat set-up has been shown before [26], one reactor run was done for each condition. The 16:8 h LD cultivation was repeated in this study and the results were comparable with our previous study for the wild-type and starchless mutant *slm1*, as shown in Supplementary Fig. S1. This shows the reproducibility of the experimental set-up.

During the light period, the cultures were diluted to maintain a constant light absorption over the culture and thus, a constant flux of photons to the culture inside the turbidostat-controlled reactors. The dilution rate for the wild-type and *slm1* mutant under the three different LD cycles are presented in Fig. 1. For the wild-type, maximum dilution rate was always reached 5–7 h after sunrise. When comparing both strains, their dilution patterns were similar (Fig. 1), where the wild-type reached higher dilution rates compared to the *slm1* mutant, indicating a faster growth rate. For the *slm1* mutant, no difference in maximum dilution rate value was found between the photoperiods 14:10 h and 12:12 h LD (0.07 h^{-1}) (Fig. 1B). However, for the 16:8 h LD cycle, the maximum value reached was higher (0.09 h^{-1}). Additionally, an unexplained oscillatory pattern was observed in this cycle for the mutant (Fig. 1B), which was also observed in previous cultures at this LD cycle (Supplementary Fig. S1).

Table 1
Comparison of average dilution rate per 24 h (D_{24h}), doubling time and dilution per hour of light supplied of *Tetradesmus obliquus* wild-type and *slm1* under 3 different light/dark cycles.

Light/dark period	Average D_{24h} (day^{-1})				Doubling time (day)		Average D over light period (day^{-1})	
	Wild-type		*slm1*		Wild-type	*slm1*	Wild-type	*slm1*
16:8	1.03	± 0.05	0.93	± 0.04	0.67	0.75	1.55	1.40
14:10	0.94	± 0.06	0.76	± 0.02	0.74	0.91	1.61	1.30
12:12	0.87	± 0.02	0.66	± 0.03	0.80	1.05	1.74	1.32

Average D_{24h} values are shown as value ± standard deviation for at least three daily values (n ≥ 3).

Table 1 shows for all conditions the average dilution rate over 24 h (D_{24h}), which is equal to the average growth rate. As can be seen, shorter light periods lead to lower dilution rates for both the wild-type and the *slm1* mutant, which is expected based on the fact that these cultures received a lower amount of light. Higher average D_{24h} translates into shorter doubling time (t_d), as the microalgae are growing faster (Table 1). By looking into the doubling times (Table 1), it can be seen that for the wild-type this value is always below one per day, indicating that at least some cells must divide more than once per day. For the *slm1*, doubling times are higher, specially under 14:10 h and 12:12 h LD cycles, indicating that cells divided approximately once per day. To verify if the difference in dilution rate can be fully explained by the difference in light received, the average dilution over the light period was calculated and is also shown in Table 1. This results in a more or less constant dilution rate for the *slm1* mutant, while the wild-type actually shows an increase in the dilution with shorter day lengths. This means that the wild-type, during the time the light is on, grows faster at shorter light periods.

The light/dark periods at which microalgae are exposed impact biomass production and metabolism of microalgae [16,39]. As microalgal biomass production would be done outdoors with natural light/dark periods, the influence of LD cycles with different lengths has been

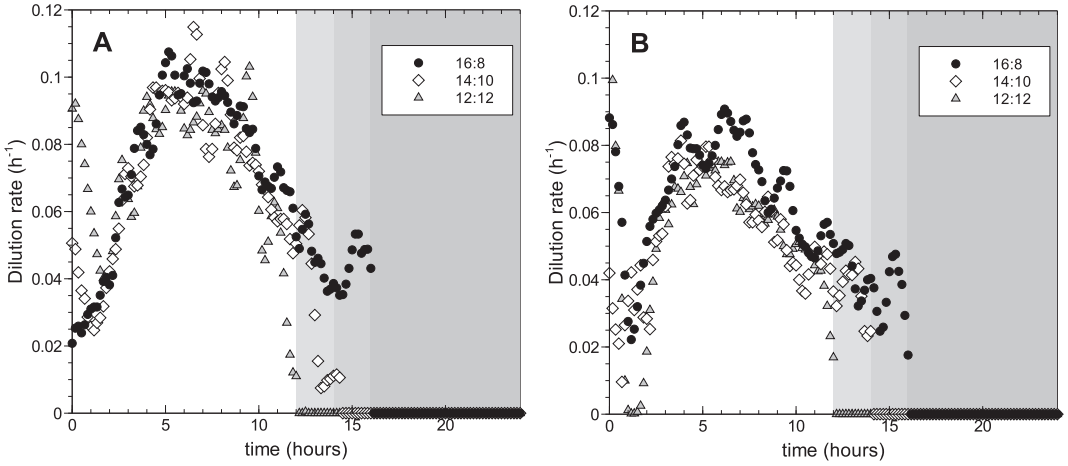

Fig. 1. Changes in dilution rate over a 24 h period for *Tetradesmus obliquus* wild-type (A) and *slm1* (B) during different photoperiods: 16:8 h light/dark (LD), 14:10 h LD and 12:12 h LD. The x axis represents hours after "sunrise". Shaded area indicates the dark period.

studied. De Winter et al. [37] studied the influence of three different LD cycles: 20:4 h, 16:8 h and 12:12 h LD on growth of the microalga *Neochloris oleoabundans* under continuous turbidostat conditions. As expected, they also observed a decrease in the average D_{24h} with the shorter light periods. Dilution patterns were comparable with the ones observed for *T. obliquus*, reaching the maximum value approximately after 6 h of light and then decreasing until the end of the light period.

Additionally, Jacob-Lopes et al. [16] studied the influence of 12 different LD periods, from continuous light (24:0 h) to 2:22 h LD, on biomass production of the cyanobacterium *Aphanothece microscopica Nägeli*. They observed a linear reduction in biomass productivity with the reduction in the length of the light period, except for the 12:12 h LD, where the value did not follow the trend and increased compared to the value at 14:10 h LD cycle. Krzeminska et al. [39] investigated the influence of light/dark cycles (12:12 h LD), compared to continuous light, on 5 different microalgae species: *Neochloris conjuncta*, *Neochloris terrestris, Neochloris texensis*, *Botryococcus braunii* and *Tetradesmus obliquus* under batch cultivation. They looked into the biomass doubling time and found that the microalgae *B. braunii* and *T. obliquus* had a higher growth rate under continuous light, while the three species of *Neochloris* grew better under 12:12 h LD cycles. The results obtained for *T. obliquus* agree with our results where the doubling time obtained under 12:12 h LD (0.80 day) was higher than that obtained by León-Saiki et al. [26] under continuous light (0.46 day). However, our values of doubling time were lower than those reported by Krzeminska et al. [39] (1.17 ± 0.02 day under 12:12 h LD and 0.93 ± 0.01 day under continuous light), which could be related to the experimental conditions (such as cultivation medium and light settings).

Growth behavior of microalgal starchless mutants varies under nitrogen replete conditions. However, most of the studies have been carried out under continuous light. The starchless mutant *BAFJ5* of *Chlamydomonas reinhardtii* showed reduced growth compared to its wild-type under continuous light [27], as was also observed for the starchless mutant of *T. obliquus slm1* under continuous light [26]. While Vonlanthen et al. [29] found no significant difference in growth for the starchless mutant *ST68* of *Chlorella sorokiniana* compared to the wild-type. For starchless mutants only one study could be found that was done under LD cycles. The growth of a starchless mutant of *Chlorella pyrenoidosa STL-PI* was studied under continuous light and a 12:12 h LD cycle [28]. The authors found a higher growth rate of the mutant compared to the wild-type for both conditions, opposite to what we found for *T. obliquus*. This could be due to differences between these two species. Another explanation could be the fact that they based their conclusions on cell numbers and not on dry weight and that the amount of dry weight per cell is lower for the mutant than for the wild-type. However, this hypothesis cannot be tested as the results on dry weight production are not presented.

3.2. Cell division

Next we looked into the differences in cell division between the strains during the different LD cycles. First, we measured cell density in intervals of 1 h (Fig. 2). Cell counts from León-Saiki et al. [26] were included together with the data obtained by repeating the 16:8 h LD cycle. All cycles showed a decrease in cell number when the light started (t = 0) for a period of about 12 h due to dilution of the reactor. Cell numbers then stayed constant for a period of 3 h after which they increased sharply from t = 15 h to t = 20 h. Cell numbers differed between the photoperiods and strains. For the wild-type under 16:8 h LD, cell density went from approximately 29.8 million cells·mL^{-1} to 61.4 million cells·mL^{-1} (Fig. 2A). For the 14:10 h LD, cell density increased from 35.5 million cells·mL^{-1} to 72.7 million cells·mL^{-1}. Finally, for the 12:12 h LD cell density was lower and increased from 28.4 million cells·mL^{-1} to 55.2 million cells·mL^{-1}. The higher cell density for the 14:10 h LD could be explained by the higher proportions in cells with lower diameter compared to the other two LD cycles (Supplementary Fig. S2A). This indicates a lower absorbance per cell possibly due to a lower pigment content. For the wild-type, in general, cell number doubled within a small time-frame between 16 and 19 h for all the tested LD cycles.

The cell densities for the *slm1* were lower than for the wild-type in all tested LD cycles (Fig. 2B). For the 16:8 h LD, cell density went from 26.1 million cells·mL^{-1} to 51.0 million cells·mL^{-1}. For the 14:10 h LD, cell density increased from 26.8 million cells·mL^{-1} to 39.4 million cells·mL^{-1}. Finally, for the 12:12 h LD cell density was lower and increased from 24.6 million cells·mL^{-1} to 43.8 million cells·mL^{-1}. While for the wild-type the increase in cell density happened within a short time frame between 15 and 19 h, for the mutant under 16:8 h LD and 12:12 h LD cycles the increase started earlier and was slower (between 14 and 21 h). For the 14:10 h LD, cell increase was faster, taking only 2 h (t = 16 h).

Since the change in cell numbers are a combined effect of cell division and dilution, we calculated the cell division rate to identify more precisely when cell division took place. For this the cell number data and the average dilution rate per hour were used, as explained in material and methods section 2.5. Fig. 3 shows the cumulative average cell division rate for a certain time (t). This is the average proliferation per day over the period from t = 0 to t = t.

For the wild-type, there is a slow cell division rate during most of the day period, as can be seen from the small slope of the curve (Fig. 3A). In general, cell division started around 14–15 h after the light went on, independently of the LD cycle, which is in accordance with the literature [37]. Cell division stops 17–18 h after the light went on. For the 16:8 h LD the sudden increase in cell division and the stop of cell division seem to start 1 h earlier than for the other two LD cycles. As expected, the final cumulative growth rate reached was comparable to the 24 h average dilution rate (D_{24h}) mentioned in Table 1 and was higher for longer light periods, which is directly related to the longer light periods.

Timing and patterns of cell division were different in the *slm1* compared to the wild-type. The slow cell division rate during the day is comparable to the wild-type. The sudden increase in cell division rate is less sharp for the *slm1* and seems to start earlier, around 10–12 h after sunrise (14–15 h for the wild-type) independent of the length of the LD cycle applied. The period to complete cell division after the sudden increase at 10–12 h is longer for the mutant (8 h) than for the wild-type (3 h) (Fig. 3B). When comparing the average cell size at the point where the sudden increase started (this is 14–15 h for the wild-type and 10–12 h for the *slm1*), we observed that the average diameter is the same for both strains (Supplementary Fig. S2C and D). This size could be an indicator of reaching the point after which cell division can occur independently of the presence of light [40]. The decreased cell division rate of the *slm1*, as well as the timing of the cell division (starting during the light period) is possibly related to the absence of a temporary energy storage compound (starch), which translates into less availability of carbon and energy.

As previously mentioned, light is one of the major cues for synchronization to daily cycles. Timing of cell division in microalgae has been suggested to depend on dawn (sunrise) and dusk (sunset) [37]. For *T. obliquus*, sunrise seems to be the factor that defines timing of cell division, since the starting of cell division was similar (approximately 14 h for the wild-type and 10–12 h for the *slm1*), independently of the beginning of the dark period.

3.3. Changes in starch content

Concomitant with the synchronization to the LD cycles, cell composition changes throughout a 24 h cycle [14,15,41,42]. As previously observed, starch is the main component that shows oscillations in *T. obliquus* wild-type during light/dark cycles [26].

As expected, starch was accumulated during the light period, and reached its maximum measured content when the night started

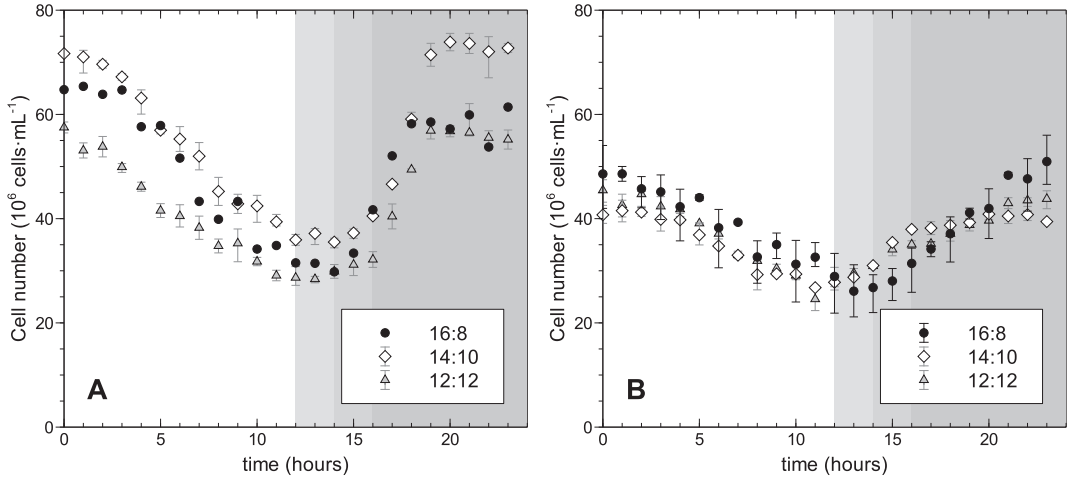

Fig. 2. Cell density over a 24 h period for *Tetradesmus obliquus* wild-type (A) and *slm1* (B). The x axis represents hours after "sunrise". Shaded areas indicate the dark periods. Error bars show the highest and lowest values found for cell counts (with 2 or more data points used, n ≥ 2), except for the wild-type under 16:8 h LD where some measurements were single and no error bars are shown. Data from León-Saiki et al. [26] is included for the 16:8 h LD period.

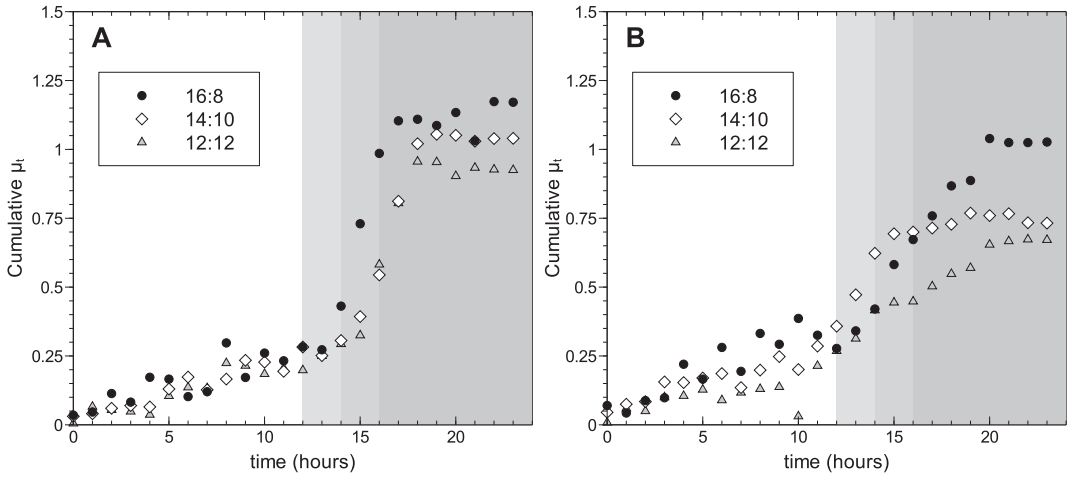

Fig. 3. Cumulative average cell division rate (μ_t) for *Tetradesmus obliquus* wild-type (A) and *slm1* (B) during different photoperiods: 16:8 h LD, 14:10 h LD and 12:12 h LD. The x axis represents hours after "sunrise". Shaded area indicates the dark period.

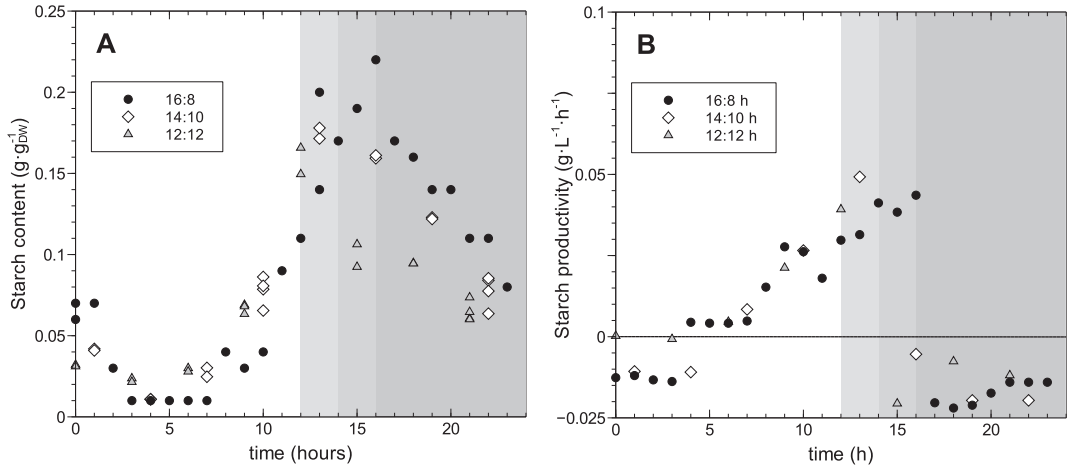

Fig. 4. Changes in starch content (A) and starch productivity (B) for *Tetradesmus obliquus* wild-type under different light/dark (LD) cycles. The x axis represents hours after "sunrise". Shaded area indicates the different dark periods. Data for the 16:8 h LD cycle was provided by León-Saiki et al. [26].

(Fig. 4A). The longer the light period, the higher the content of starch (0.22 $g \cdot g_{DW}^{-1}$ for the 16:8 h LD, 0.18 $g \cdot g_{DW}^{-1}$ for the 14:10 h LD and 0.16 $g \cdot g_{DW}^{-1}$ for the 12:2 h LD cycle). In all LD cycles, starch content started increasing approximately 7 h after sunrise (Fig. 4A). A similar behavior was observed for the microalga *Neochloris oleoabundans* [37], where starch content started to increase 6–7 h after "sunrise", with a higher maximum starch content with longer photoperiods.

To study the changes in starch production/consumption, we calculated the starch productivity during the measured time points (Fig. 4B). Starch production rate started and increased about 5–7 h after the light went on. As soon as the dark period started, starch was consumed. As the light went on again starch consumption continued until 4 h after sunrise. After this time point starch was depleted for the 16:8 h LD and 14:10 h. A notable exception was the 12:12 h LD showing no consumption in these 4 h; also, the starch content did not become zero. It is unclear why *T. obliquus* did not totally consume the stored starch under this LD cycle, however, it should be mentioned that starch content was measured in intervals of 3 h, and the point where starch is completely used as well as starch consumption may have been missed at this low resolution of measurements. Interestingly, the moment when starch is depleted coincides with the maximum value of the dilution rate (Fig. 1A). At this maximum dilution rate, starch consumption switches to starch production (around 8 h after sunrise).

The non-starch carbohydrates showed no changes through the measured points (Supplementary Fig. S3). The protein content for the wild-type showed a decrease during the light period, which was concomitant with the increase in starch content (Supplementary Fig. S3). For both strains, TAG content remained below 0.01 $g \cdot g_{DW}^{-1}$ in all sampling points (not shown). For the starchless mutant *slm1*, starch levels remained below 0.016 $g \cdot g_{DW}^{-1}$ during all sampled points in all photoperiods tested (not shown) and no fluctuations in biomass composition were observed for the tested LD cycles (Supplementary Fig. S3).

3.4. Efficiency of energy fixation in biomass components

To calculate the energy conversion efficiency, i.e. the fraction of photons absorbed whose energy is fixed in biomass components, we measured the biomass composition (functional biomass and storage compounds, i.e. starch) of the daily overflows for both strains. The overflow composition remained similar during the different LD cycles (Table 2), but the average dry weight concentration, as well as the biomass productivity showed an increase with longer light periods. The TAG fraction was low (below 0.01 $g \cdot g_{DW}^{-1}$) and therefore not considered for the calculations. For *T. obliquus* wild-type a similar fraction of the supplied energy was fixed in biomass under 14:10 h (54.61 ± 0.07%) and 12:12 h (55.18 ± 0.06%) LD cycles (Fig. 5A). These values were lower compared to the 16:8 h LD cycle (62.77 ± 0.08%). This could be related to timing of cell division. The 16:8 h LD cycle is the only one where cell division starts during the day. Thus part of the energy needed for cell division may still come from the light, resulting in less use of starch during the night and allowing to fix extra energy compared to 14:10 h and 12:12 h LD, where cell division occurs at night and relies completely on starch.

For the wild-type, the biomass yield on light was the highest with the longest light period (16:8 h LD) (Table 2). However, the increase does not continue until the dark period is skipped (continuous light), as the biomass yield on light was 0.98 ± 00 $g \cdot mol_{ph}^{-1}$ [26].

When the starch synthesis path is blocked, as in the *slm1* mutant, the energy efficiency is lower than for the wild-type for all LD cycles (Fig. 5A). However, the behavior was different compared to its wild-type. For the mutant, the highest biomass yield on light and the energy conversion efficiency occurred under 16:8 h LD cycle. This was surprisingly maintained during the 14:10 h LD, but dropped for the longest dark period tested (12:12 h LD cycle) (Table 2). This could also be related to timing of cell division. The 12:12 h LD cycle is the only tested photoperiod where cell division occurs mainly in the dark. This agrees with the slower division rates observed for this cycle compared to 16:8 h and 14:10 h LD where cell division starts during the day (Fig. 3).

During a LD cycle the dilution rate and biomass composition changed. Since the photon absorption rate is constant, the energy conversion efficiency will change over a LD cycle. To get more insight into this, the energy efficiency was calculated in one hour intervals based on the measured biomass composition, dilution rate and photon absorption rate at each time point. By looking at the energy conversion efficiency during the daily cycles, we found that the highest energy fixation occurs with the maximum dilution rate (Fig. 5B and C). Both strains showed similar patterns but, as expected, the wild-type reached higher values (approximately 90%) compared to the starchless mutant *slm1* (maximum 80%). This maximum value decreased slightly with the shorter light periods for both the mutant and wild-type.

At the start of the day starch is still used. Probably this is for the rapid synthesis of absorbing material to harvest the light energy, which can be deduced from the rapid increase in dilution rate. Depletion of the starch coincides with the maximum energy efficiency and dilution rate. From that moment on starch is net synthesized and the starch content increases again. During the night, the starch is used again for cell division and preparation for the moment when light goes on again. This can be derived from the fact that cell division is much slower in the mutant and the fact that for the mutant the increase in dilution rate starts later after the light is turned on. Apparently, starch is used during the night to prepare for the next light cycle or during the night energy is derived from cell components that have to be built up again if the light goes on.

4. Conclusions

The start of the light phase (sunrise) is the reference point for synchronized cell division in *Tetradesmus obliquus*. Cell division in *T. obliquus* wild-type started approximately 14 h after sunrise, independently of the length of the light period. Cell division occurred mainly at night, except during the longest light period tested (16:8 h

Table 2
Average steady state values for *Tetradesmus obliquus* wild-type and *slm1* under different light/dark cycles.

	Wild-type			*slm1*		
	16:8	14:10	12:12	16:8	14:10	12:12
Dry weight concentration ($g \cdot L^{-1}$)	1.38 ± 0.07	1.15 ± 0.07	1.07 ± 0.04	1.18 ± 0.05	1.23 ± 0.03	1.07 ± 0.02
Biomass productivity ($g \cdot L^{-1} \cdot day^{-1}$)	1.42 ± 0.08	1.08 ± 0.07	0.93 ± 0.04	1.10 ± 0.07	0.94 ± 0.03	0.70 ± 0.03
Biomass yield on light ($g \cdot mol_{ph}^{-1}$)	1.04 ± 0.08	0.91 ± 0.09	0.91 ± 0.04	0.81 ± 0.07	0.79 ± 0.04	0.68 ± 0.03
Starch ($g \cdot g_{DW}^{-1}$)	0.05[a] ± 0.01	0.05 ± 0.01	0.03 ± 0.01	0[a]	0	0
Photon absorption rate ($mol_{ph} \cdot L^{-1} \cdot day^{-1}$)	1.36	1.19	1.02	1.36	1.19	1.02

Average values are shown as value ± standard deviations. Standard deviations were calculated based on at least 3 overflows. Except for the wild-type under 12:12 h LD where n = 2, and the value represents the average ± max/min values.

[a] Values taken from León-Saiki et al., [26].

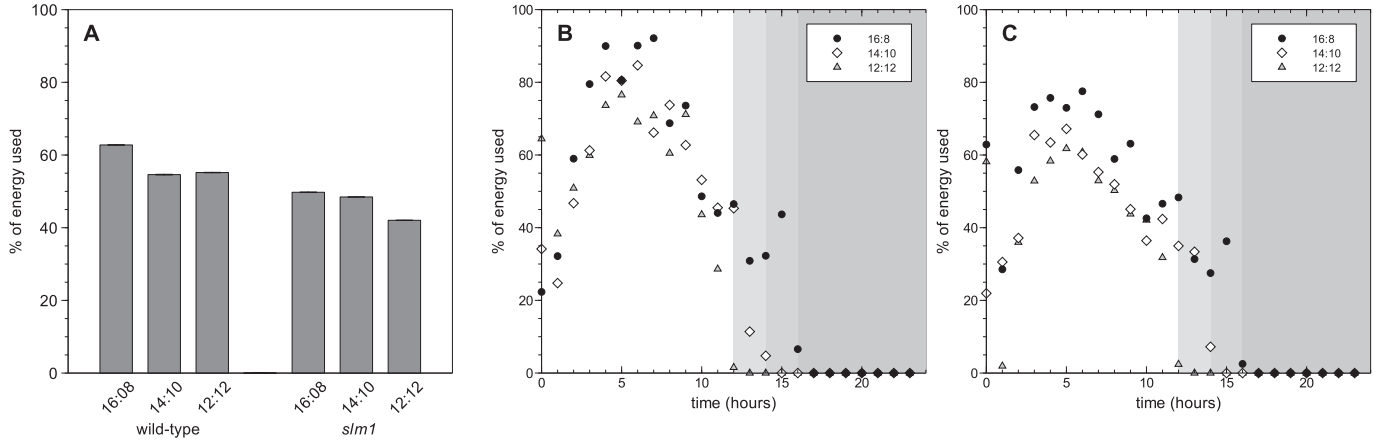

Fig. 5. Theoretical photon efficiency as percentage of photons used to make biomass components (A) and hourly percentage of photons used for *Tetradesmus obliquus* wild-type (B) and *slm1* (C) under different light/dark (LD) cycles. Values represent averages of at least 3 daily overflows for (A). Error bars represent the standard deviations calculated by error propagation. For the hourly energy conversion efficiency the x axis represents hours after "sunrise". Shaded area indicates the dark period. Data for the 16:8 h LD cycle was provided by León-Saiki et al. [26].

light/dark cycle), where cell division started at the end of the light period and extended into the dark period. For the *slm1* mutant, cell division was also synchronized to the start of the light period but started earlier than for the wild-type (10–12 h after sunrise). Regarding biomass composition, the length of the day had an influence on the maximum starch content reached by the wild-type: the longer the light period, the higher the starch content. The starchless mutant *slm1* showed no oscillations in biomass composition. But, despite the lack of starch, the *slm1* mutant synchronized growth and cell division to the LD cycles. However, the absence of starch resulted in lower energy efficiencies (11–24% lower) and biomass yield on light (13–39% lower) for *T. obliquus slm1* compared to its wild-type under all tested LD cycles.

Author contributions

GMLS, DV, and DEM conceived the research and designed the experiments; GMLS and TCM performed the experiments, analyzed and interpreted the data. GMLS wrote the article. DV, RHW and DEM supervised and edited the manuscript. All authors read and approved the final manuscript.

Funding information

This research project was supported by the Consejo Nacional de Ciencia y Tecnología – CONACYT, Mexico, Scholar 218586/Scholarship 314173. In addition, GMLS is part of the program "Doctores Jóvenes para el Desarrollo Estratégico Institucional" by the Universidad Autónoma de Sinaloa.

Conflict of interest

The authors declare no conflict of interest.

Statement of informed consent, human/animal rights

No conflicts, informed consent, human or animal rights applicable.

Appendix A. Supplementary data

Supplementary data to this article can be found online at https://doi.org/10.1016/j.algal.2018.02.027.

References

[1] R.H. Wijffels, M.J. Barbosa, M.H.M. Eppink, Microalgae for the production of bulk chemicals and biofuels, Biofuels Bioprod. Biorefin. 4 (2010) 287–295, http://dx.doi.org/10.1002/bbb.215.
[2] R.H. Wijffels, M.J. Barbosa, An outlook on microalgal biofuels, Science 329 (2010) 796–799, http://dx.doi.org/10.1126/science.1189003.
[3] W. Blanken, M. Cuaresma, R.H. Wijffels, M. Janssen, Cultivation of microalgae on artificial light comes at a cost, Algal Res. 2 (2013) 333–340, http://dx.doi.org/10.1016/j.algal.2013.09.004.
[4] N.-H. Norsker, M.J. Barbosa, M.H. Vermuë, R.H. Wijffels, Microalgal production — a close look at the economics, Biotechnol. Adv. 29 (2011) 24–27, http://dx.doi.org/10.1016/j.biotechadv.2010.08.005.
[5] L.P. Shearman, S. Sriram, D.R. Weaver, E.S. Maywood, I. Chaves, B. Zheng, K. Kume, C.C. Lee, G.T.J. van Der, M.H. Hastings Horst, S.M. Reppert, Interacting molecular loops in the mammalian circadian clock, Science 288 (2000) 1013–1019, http://dx.doi.org/10.1126/science.288.5468.1013.
[6] H.C. Causton, K.A. Feeney, C.A. Ziegler, J.S. O'Neill, Metabolic cycles in yeast share features conserved among circadian rhythms, Curr. Biol. 25 (2015) 1056–1062, http://dx.doi.org/10.1016/j.cub.2015.02.035.
[7] L. Salichos, A. Rokas, The diversity and evolution of circadian clock proteins in fungi, Mycologia 102 (2010) 269–278, http://dx.doi.org/10.3852/09-073.
[8] C.R. McClung, Plant circadian rhythms, Plant Cell 18 (2006) 792–803, http://dx.doi.org/10.1105/tpc.106.040980.
[9] M. Mittag, Circadian rhythms in microalgae, B.-I.R. of Cytology, Academic Press, 2001, pp. 213–247 http://www.sciencedirect.com/science/article/pii/S0074769601060235 (accessed May 13, 2016).
[10] Y. Niwa, T. Matsuo, K. Onai, D. Kato, M. Tachikawa, M. Ishiura, Phase-resetting mechanism of the circadian clock in *Chlamydomonas reinhardtii*, Proc. Natl. Acad. Sci. 110 (2013) 13666–13671, http://dx.doi.org/10.1073/pnas.1220004110.
[11] T. Roenneberg, R.G. Foster, Twilight times: light and the circadian system, Photochem. Photobiol. 66 (1997) 549–561, http://dx.doi.org/10.1111/j.1751-1097.1997.tb03188.x.
[12] L. Suzuki, C.H. Johnson, Algae know the time of day: circadian and photoperiodic programs, J. Phycol. 37 (2001) 933–942, http://dx.doi.org/10.1046/j.1529-8817.2001.01094.x.
[13] S.S. Nikaido, C.H. Johnson, Daily and circadian variation in survival from ultraviolet radiation in *Chlamydomonas reinhardtii*, Photochem. Photobiol. 71 (2000) 758–765, http://dx.doi.org/10.1562/0031-8655(2000)0710758DACVIS2.0.CO2.
[14] L. de Winter, A.J. Klok, M. Cuaresma Franco, M.J. Barbosa, R.H. Wijffels, The synchronized cell cycle of *Neochloris oleoabundans* and its influence on biomass composition under constant light conditions, Algal Res. 2 (2013) 313–320, http://dx.doi.org/10.1016/j.algal.2013.09.001.
[15] J. Fábregas, A. Maseda, A. Domínguez, M. Ferreira, A. Otero, Changes in the cell composition of the marine microalga, *Nannochloropsis gaditana*, during a light:dark cycle, Biotechnol. Lett. 24 (2002) 1699–1703, http://dx.doi.org/10.1023/A:1020661719272.
[16] E. Jacob-Lopes, C.H.G. Scoparo, L.M.C.F. Lacerda, T.T. Franco, Effect of light cycles (night/day) on CO2 fixation and biomass production by microalgae in photobioreactors, Chem. Eng. Process. Process Intensif. 48 (2009) 306–310, http://dx.doi.org/10.1016/j.cep.2008.04.007.
[17] L. Krienitz, C. Bock, Present state of the systematics of planktonic coccoid green algae of inland waters, Hydrobiologia 698 (2012) 295–326, http://dx.doi.org/10.1007/s10750-012-1079-z.
[18] M.J. Wynne, J.K. Hallan, Reinstatement of Tetradesmus G. M. Smith (Sphaeropleales, Chlorophyta), Feddes Repert. 126 (2015) 83–86, http://dx.doi.org/10.1002/fedr.201500021.
[19] G. Breuer, P.P. Lamers, D.E. Martens, R.B. Draaisma, R.H. Wijffels, Effect of light

intensity, pH, and temperature on triacylglycerol (TAG) accumulation induced by nitrogen starvation in *Scenedesmus obliquus*, Bioresour. Technol. 143 (2013) 1–9, http://dx.doi.org/10.1016/j.biortech.2013.05.105.
[20] S.-H. Ho, C.-Y. Chen, J.-S. Chang, Effect of light intensity and nitrogen starvation on CO2 fixation and lipid/carbohydrate production of an indigenous microalga *Scenedesmus obliquus* CNW-N, Bioresour. Technol. 113 (2012) 244–252, http://dx.doi.org/10.1016/j.biortech.2011.11.133.
[21] S. Mandal, N. Mallick, Microalga Scenedesmus obliquus as a potential source for biodiesel production, Appl. Microbiol. Biotechnol. 84 (2009) 281–291, http://dx.doi.org/10.1007/s00253-009-1935-6.
[22] I.M. Remmers, A. Hidalgo-Ulloa, B.P. Brandt, W.A.C. Evers, R.H. Wijffels, P.P. Lamers, Continuous versus batch production of lipids in the microalgae *Acutodesmus obliquus*, Bioresour. Technol. 244 (2017) 1384–1392, http://dx.doi.org/10.1016/j.biortech.2017.04.093.
[23] L. de Jaeger, R.E. Verbeek, R.B. Draaisma, D.E. Martens, J. Springer, G. Eggink, R.H. Wijffels, Superior triacylglycerol (TAG) accumulation in starchless mutants of *Scenedesmus obliquus*: (I) mutant generation and characterization, Biotechnol. Biofuels. 7 (2014) 69, http://dx.doi.org/10.1186/1754-6834-7-69.
[24] L. de Jaeger, Strain Improvement of Oleaginous Microalgae, Bioprocess Engineering, Wageningen UR, (2015).
[25] G. Breuer, L. de Jaeger, V.P.G. Artus, D.E. Martens, J. Springer, R.B. Draaisma, G. Eggink, R.H. Wijffels, P.P. Lamers, Superior triacylglycerol (TAG) accumulation in starchless mutants of *Scenedesmus obliquus*: (II) evaluation of TAG yield and productivity in controlled photobioreactors, Biotechnol. Biofuels. 7 (2014) 1–11, http://dx.doi.org/10.1186/1754-6834-7-70.
[26] G.M. León-Saiki, I.M. Remmers, D.E. Martens, P.P. Lamers, R.H. Wijffels, D. van der Veen, The role of starch as transient energy buffer in synchronized microalgal growth in *Acutodesmus obliquus*, Algal Res. 25 (2017) 160–167, http://dx.doi.org/10.1016/j.algal.2017.05.018.
[27] Y. Li, D. Han, G. Hu, M. Sommerfeld, Q. Hu, Inhibition of starch synthesis results in overproduction of lipids in *Chlamydomonas reinhardtii*, Biotechnol. Bioeng. 107 (2010) 258–268, http://dx.doi.org/10.1002/bit.22807.
[28] A. Ramazanov, Z. Ramazanov, Isolation and characterization of a starchless mutant of *Chlorella pyrenoidosa* STL-PI with a high growth rate, and high protein and polyunsaturated fatty acid content, Phycol. Res. 54 (2006) 255–259, http://dx.doi.org/10.1111/j.1440-1835.2006.00416.x.
[29] S. Vonlanthen, D. Dauvillée, S. Purton, Evaluation of novel starch-deficient mutants of *Chlorella sorokiniana* for hyper-accumulation of lipids, Algal Res. 12 (2015) 109–118, http://dx.doi.org/10.1016/j.algal.2015.08.008.
[30] V.H. Work, R. Radakovits, R.E. Jinkerson, J.E. Meuser, L.G. Elliott, D.J. Vinyard, L.M.L. Laurens, G.C. Dismukes, M.C. Posewitz, Increased lipid accumulation in the *Chlamydomonas reinhardtii* sta7-10 Starchless Isoamylase mutant and increased carbohydrate synthesis in complemented strains, Eukaryot. Cell 9 (2010) 1251–1261, http://dx.doi.org/10.1128/EC.00075-10.
[31] Y. Li, D. Han, G. Hu, D. Dauvillee, M. Sommerfeld, S. Ball, Q. Hu, *Chlamydomonas* starchless mutant defective in ADP-glucose pyrophosphorylase hyper-accumulates triacylglycerol, Metab. Eng. 12 (2010) 387–391, http://dx.doi.org/10.1016/j.ymben.2010.02.002.
[32] A.M.J. Kliphuis, A.J. Klok, D.E. Martens, P.P. Lamers, M. Janssen, R.H. Wijffels, Metabolic modeling of *Chlamydomonas reinhardtii*: energy requirements for photoautotrophic growth and maintenance, J. Appl. Phycol. 24 (2012) 253–266, http://dx.doi.org/10.1007/s10811-011-9674-3.
[33] P.R. Postma, T.L. Miron, G. Olivieri, M.J. Barbosa, R.H. Wijffels, M.H.M. Eppink, Mild disintegration of the green microalgae *Chlorella vulgaris* using bead milling, Bioresour. Technol. 184 (2015) 297–304, http://dx.doi.org/10.1016/j.biortech.2014.09.033.
[34] M. DuBois, K.A. Gilles, J.K. Hamilton, P.A. Rebers, F. Smith, Colorimetric method for determination of sugars and related substances, Anal. Chem. 28 (1956) 350–356, http://dx.doi.org/10.1021/ac60111a017.
[35] D. Herbert, P.J. Phipps, R.E. Strange, Chemical analysis of microbial cells, Methods Microbiol, Academic Press, London and New York, 1971, pp. 209–344.
[36] K. Bišová, V. Zachleder, Cell-cycle regulation in green algae dividing by multiple fission, J. Exp. Bot. (2014) ert466, , http://dx.doi.org/10.1093/jxb/ert466.
[37] L. de Winter, I.T.D. Cabanelas, A.N. Órfão, E. Vaessen, D.E. Martens, R.H. Wijffels, M.J. Barbosa, The influence of day length on circadian rhythms of *Neochloris oleoabundans*, Algal Res. 22 (2017) 31–38, http://dx.doi.org/10.1016/j.algal.2016.12.001.
[38] G. Breuer, P.P. Lamers, M. Janssen, R.H. Wijffels, D.E. Martens, Opportunities to improve the areal oil productivity of microalgae, Bioresour. Technol. 186 (2015) 294–302, http://dx.doi.org/10.1016/j.biortech.2015.03.085.
[39] I. Krzemińska, B. Pawlik-Skowrońska, M. Trzcińska, J. Tys, Influence of photoperiods on the growth rate and biomass productivity of green microalgae, Bioprocess Biosyst. Eng. 37 (2014) 735–741, http://dx.doi.org/10.1007/s00449-013-1044-x.
[40] H. Oldenhof, V. Zachleder, H. van den Ende, The cell cycle of *Chlamydomonas reinhardtii*: the role of the commitment point, Folia Microbiol. (Praha). 52 (2007) 53, http://dx.doi.org/10.1007/BF02932138.
[41] M.S. Chauton, P. Winge, T. Brembu, O. Vadstein, A.M. Bones, Gene regulation of carbon fixation, storage, and utilization in the diatom *Phaeodactylum tricornutum* acclimated to light/dark cycles, Plant Physiol. 161 (2013) 1034–1048, http://dx.doi.org/10.1104/pp.112.206177.
[42] E. Poliner, N. Panchy, L. Newton, G. Wu, A. Lapinsky, B. Bullard, A. Zienkiewicz, C. Benning, S.-H. Shiu, E.M. Farré, Transcriptional coordination of physiological responses in *Nannochloropsis oceanica* CCMP1779 under light/dark cycles, Plant J. 83 (2015) 1097–1113, http://dx.doi.org/10.1111/tpj.12944.